Research Article

Journal of Oil and Gas Research Reviews

Multiobjective nonlinear model predictive control of microalgal culture processes

Lakshmi. N. Sridhar*

Chemical Engineering Department, University of Puerto Rico, Mayaguez, PR 00681.

***Corresponding Author**
Lakshmi. N. Sridhar, Chemical Engineering Department, University of Puerto Rico, Mayaguez, PR 00681.

Submitted: 2023, Nov 02; **Accepted:** 2023, Nov 21; **Published:** 2023, Dec 01

Citation: Sridhar, L. N. (2023). Multiobjective nonlinear model predictive control of microalgal culture processes. *J Oil Gas Res Rev, 3*(2), 119-133.

Abstract

A rigorous multiobjective nonlinear model predictive control strategy was used for dynamic models involving the microalgae culture process. The models are the droop model, the nitrogen limited microalgae culture process model, and the Thornton model. It was shown that the implementation of the NLMPC method causes an increase in algal growth. The optimization language pyomo is used in conjunction with the state-of-the-art global optimization solvers IPOPT and BARON. Pareto surfaces are generated. When some optimal control profiles were found to exhibit sharp spikes, an activation factor involving the hyperbolic cotangent function was used to eliminate the inconvenient spikes.

Keywords: Microalgae, Optimization, Control.

1. Introduction

The benefits of producing biodiesel from microalgae are well-known and welldocumented. These benefits arise from both productivity and sustainability. The production of biodiesel from microalgae is both sustainable and beneficial. It has been shown that the oil productivity of microalgae is much higher than the oil productivity of many other crops [1-11]. At this time, microalgae seem to be the primary source of biodiesel that can meet the growing need for energy. Microalgae are small-size biochemical industries as they consume nutrients to grow. There has been a considerable amount of modeling work by. Thornton, Weinhart, Bokhove Zhang., Sar, Kuma., Pisarenco, Rudnaya., Sacenco, Rademacher., ijlstra., Szabelska., Zyprych, Schans., Timperio, Daneerman], provided a model that considered the microalgae harvest rate and death rate. The effect of light and nutrients caused the development of the more complex nitrogen-limited microalgae culture process [MCP] model [12-14].

This model was discussed in detail by Bernard and co-workers [16]. The research of Thornton et al [15] and Bernard et al [16] demonstrate that there is more than one factor that plays a role in the growth of microalgae. The aim of this work is to therefore perform multiobjective nonlinear model predictive control on the three models 1) the Droop model 2) the Thornton model and 3) the microalgae culture process [MCP] model. The paper is organized as follows. First, the three models are described. This is followed by a description of the multiobjective nonlinear model predictive control procedure. The results and discussion are then presented, followed by the conclusions.

1.2. Droop Model

The Droop model is very commonly used to demonstrate the microalgal culture dynamics and consists of three equations [12, 13]:

$$\frac{ds}{dt} = D(t)S_{in}(t) - \rho(S(t))x - D(t)S(t) \quad (1)$$

$$\frac{dq}{dt} = \rho(S(t)) - \mu(q(t))q \quad (2)$$

$$\frac{dX}{dt} = \mu(q(t))X(t) - D(t)X(t) \quad (3)$$

Here X represents the biomass, S the concentration of the limiting nutrient [e.g., a nitrogen limitation induces lipid synthesis], q is the internal nitrogen cell quota which is defined by the amount of nitrogen per biomass cell unit, D is the dilution rate, in S_{in} is the influent inorganic nitrogen concentration and the growth rate of the biomass. The absorption rates $P(S(t))$ is represented by Michaelis Menton kinetics

$$\rho(S(t)) = \rho_m \frac{S(t)}{S(t) + K_s} \quad (4)$$

whereas the maximum uptake rate and the half-saturation constant for substrate uptake. The growth rate $\mu(q)$ is based on the Droop function

$$\mu(q(t)) = \bar{\mu}(1 - \frac{Q_0}{q(t)}) \quad (5)$$

μ is the growth rate at a hypothetical infinite quota and is the minimal cell quota for which no algal growth can take place? The units of X and S are in g/L, while the units of μ, d, p are day $^{-1}$. The parameter values are p_m= 0 0.1 μ = 1.645, 0.04, q_m=0.04, K_s=7.5. The two control variables are D (0.1 -1) the dilution rate, and in S_{in} (30-100) the influent inorganic nitrogen concentration.

1.3. Nitrogen Limited MCP model

The Nitrogen limited MCP model [Bernard] accounts for the response of microalgal pigment density to both light intensity and available nutrients [16]. The equations that constitute this model are

$$\frac{ds}{dt} = D(t)S_{in}(t) - \bar{\rho}\left(\frac{s(t)}{s(t)+K_s}\right)\left(1-\frac{q(t)}{Q_l}\right)x(t) - D(t)s(t) \quad (6)$$

$$\frac{dq}{dt} = \bar{\rho}\left(\frac{s(t)}{s(t)+K_s}\right)\left(1-\frac{q(t)}{Q_l}\right) - \bar{\mu}(q(t)-Q_0) \quad (7)$$

$$\frac{dx}{dt} = \bar{\mu}\left(1-\frac{Q_0}{q}\right)x(t) - Dx(t) - Rx(t) \quad (8)$$

$$\frac{dI^*}{dt} = \bar{\mu}\left(1-\frac{Q_0}{q(t)}\right)\left(\bar{I}(t) - I^*(t)\right) = 0 \quad (9)$$

$$\gamma = \gamma_{\max}\left(\frac{K_i}{K_i + I^*(t)}\right) \quad (10)$$

$$\bar{I}(t) = I_0(t)\frac{K_g}{K_g + (\gamma(t)aq(t)x(t)+b)l} \quad (11)$$

Here X represents the biomass, S the concentration of the limiting nutrient [e.g., a nitrogen limitation induces lipid synthesis], q is the internal nitrogen cell quota which is defined by the amount of nitrogen per biomass cell unit, D is the dilution rate, S_m is the influent inorganic nitrogen concentration and the growth rate of the biomass. I_0 irradiance at the surface. The units of X and S are in g/L, while the units of μ, p ,d, are day^{-1}. I*(μmoml^{-2}s^{-1}) is the irradiance at which the cells are photo-acclimated and in a light homogeneous steady-state culture, this variable is exactly the mean radiance I(μmoml^{-2}s$_{-1}$). Q_1 is the upper limit for q and R is the respiration rate. A detailed description of all the parameters in the nitrogen limited MCP model is present in Bernard et al [16]. The parameter values and units are presented in table 1.

Parameter	Value	units
$\bar{\mu}$	1.6	Day^{-1}
Q_0	0.053	gNgC^{-1}
Q_l	0.11	gNgC^{-1}
$\bar{\rho}$	0.1	gNgC^{-1} Day^{-1}
K_g	1.25	$\mu molm^{-2}s^{-1}$
K_s	50	gNm^{-3}
R	0.0081	day^{-1}
a	16.2	m2 gChl^{-1}
b	0.087	m^{-1}
l	0.054	m
$\gamma_{\max}$	0.12	gChl^{-1}m^2

Table:1

1.4. Thornton Model

The Thornton model [Thornton, A., Weinhart, T., Bokhove, O., Zhang, B., Sar, D.M. v. d., Kumar, K., Pisarenco, M., Rudnaya, M., Sacenco, V., Rademacher, J., ijlstra, J., Szabelska, A., Zyprych, j., Schans, M.v.d., Timperio, V. daneerman, F. and Setyowati, Suci and Mardlijah, Mardlijah, describes algal growth that is influenced by carbon dioxide concentration, nutrients, and glucose [15, 17]. Carbon dioxide is fed into the water and is converted into glucose by photosynthesis. The algae are additionally reduced because of harvest and death. The equations governing the Thornton model are

$$\frac{dA}{dt} = \rho_{\max}\left(\frac{M(t)}{M(t)+M_t urn}\right)\alpha_A S(t) - (d_r + h_r)A(t) \tag{12}$$

$$\frac{dM}{dt} = -\rho_{\max}\left(\frac{M(t)}{M(t)+M_t urn}\right)k_2\alpha_A S(t) + I_m(t) \tag{13}$$

$$\frac{dS}{dt} = -\rho_{\max}\left(\frac{M(t)}{M(t)+M_t urn}\right)k_3\alpha_A S(t) - (d_r + h_r)A(t) + \alpha_S C(t) \tag{14}$$

$$\frac{dC}{dt} = -k_1\alpha_s C(t) + I_c(t) \tag{15}$$

A is the concentration of Algae, M is the nutrient concentration, and S and C represent the concentrations of glucose and carbon dioxide. I_m and represent the inflow of nutrients and carbon dioxide while M1urn (value = 4) is the half-saturation constant for nutrient concentration inside algae. d_r (value = 0.46) and h_r (value =2) represent the harvest and death rates of the algae. The maximal nutrient concentration inside algae, p_{max} = 0.4. The rate constant for biomass growth and the rate constant for photosynthesis, α_A, α_S are 10.2 and 67.6 respectively. The constants k_1 k_2 k_3 are 0.4, 0.05 and 0.05

2. Methodology [MNLMC method]

The multiobjective nonlinear optimal control [MOOC] method was first proposed by Flores Tlacuahuaz, Pilar and Toledo and used by Sridhar [18, 19]. This method does not involve the use of weighting functions nor does it impose additional constraints on the problem unlike the weighted function or the epsilon correction method [20]. For a problem that is posed as

$$\begin{aligned} &\min J(x,u) = (x_1, x_2 .... x_k) \\ &subject\ to\ \ \frac{dx}{dt} = F(x,u) \\ &h(x,u) \le 0 \\ &x^L \le x \le x^U \\ &u^L \le u \le u^U \end{aligned} \tag{16}$$

The MNLMPC method first solves dynamic optimization problems independently minimizing/maximizing each x_i individually. The minimization/maximization of x_i*. Then the optimization problem that will be solved is

$$\begin{aligned} &\min \sqrt{\{x_i - x_i^*\}^2} \\ &subject\ to\ \ \frac{dx}{dt} = F(x,u) \\ &h(x,u) \le 0 \\ &x^L \le x \le x^U \\ &u^L \le u \le u^U \end{aligned} \tag{17}$$

This will provide the control values for various times. The first obtained control value is implemented and the remaining discarded. This procedure is repeated until the implemented and the first obtained control value are the same. The optimization package in Python, Pyomo (Hart., Laird, Watson. Woodruff, Hackebeil), where the differential equations are automatically converted to a Nonlinear Program [NLP] using the orthogonal collocation method [21, 22]. The LagrangeRadau quadrature with three collocation points is used and 10 finite elements are chosen to solve the optimal control problems. The resulting nonlinear optimization problem was solved using the solvers IPOPT [23, 24]. BARON implements a Branch-and-reduce strategy to provide valid lower and upper bounds for the optimal solution and provides a guaranteed global optimal solution. This algorithm combines constraint propagation, interval analysis, and the duality in it reduces arsenal with enhanced branch and bound concepts as it winds its way through the hills and valleys of complex optimization problems in search of global solutions. To summarize the steps of the algorithm are as follows

• Minimize/maximize x_i subject to the differential and algebraic equations that govern the process using Pyomo with IPOPT and Baron. This will lead to the value x_i* at various time intervals t_i. The subscript i is the index for each time step.

• Minimize $\sqrt{\{x_i - x_i^*\}^2}$ subject to the differential and algebraic equations that govern the process using Pyomo with IPOPT and Baron. This will provide the control values for various times.

• Implement the first obtained control values and discard the remaining.

• Repeat steps 1 to 4 until there is an insignificant difference between the implemented and the first obtained value of the control variables.

3. Results and Discussion

3.1. Droop model

For the multiobjective nonlinear model predictive control of the droop model, the control variables are S_{in} and d. $\sum x_i$ *and* $\sum \mu_i$ are maximized individually which leads to the values 46.6396 and 1.779 respectively. The new optimization problem would be the minimization of the function $\sqrt{(\sum x_i - 46.6396)^2 + (\sum \mu_i - 1.779)^2}$ subject the equations 1-5. The obtained NLMPC values of S_{in} and d were 100 and 0.78. Here, figs 1-7 represent the variation of the variables with time while figs 8-10 represent the Pareto surfaces. Fig. 2 and Fig. 5 show the variation of the control variables d and S_{in} the NLMPC strategy demonstrates an increase in both x and μ (figs 1 and 4).

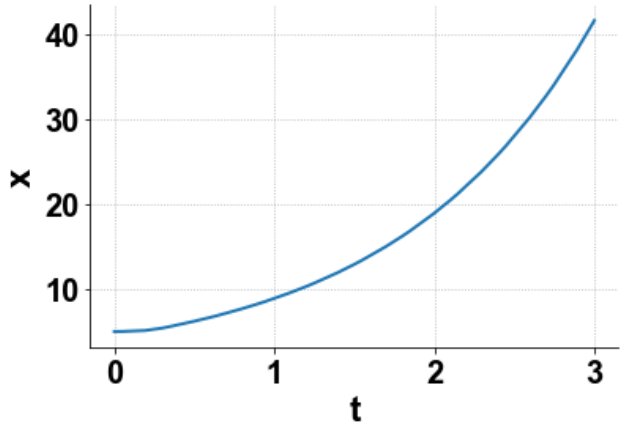

Figure 1: Droop model x versus t

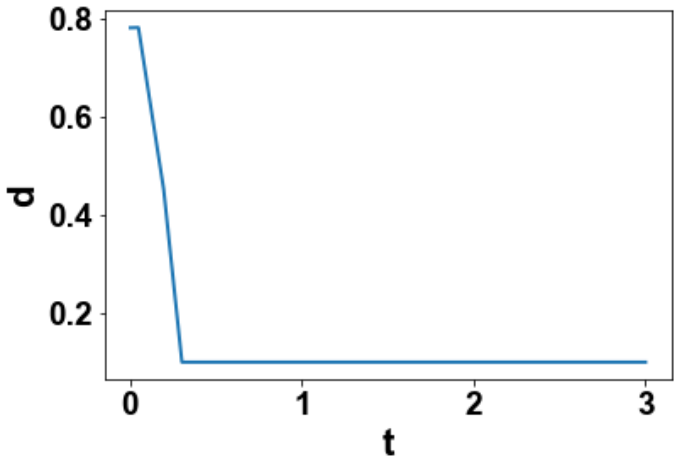

Figure 2: Droop model d versus t

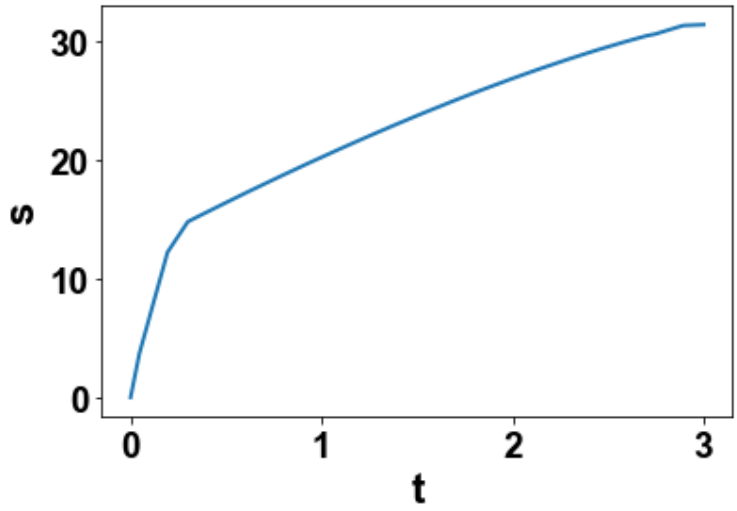

Figure 3: Droop model x versus t

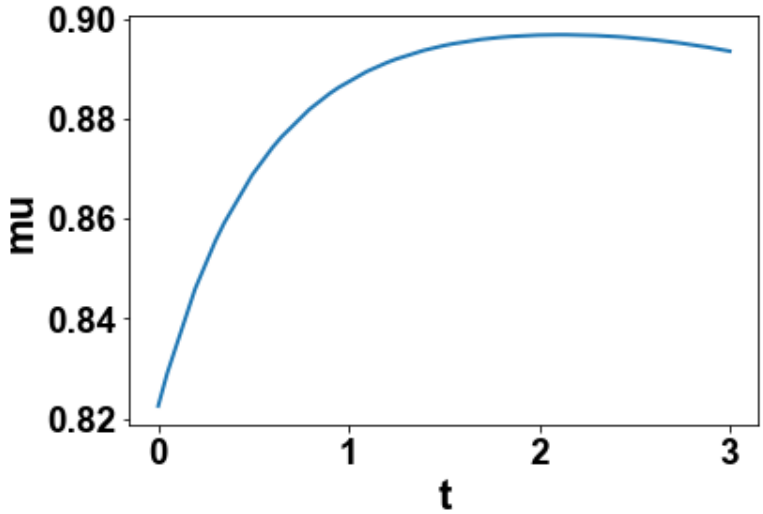

Figure 4: Droop model mu versus t

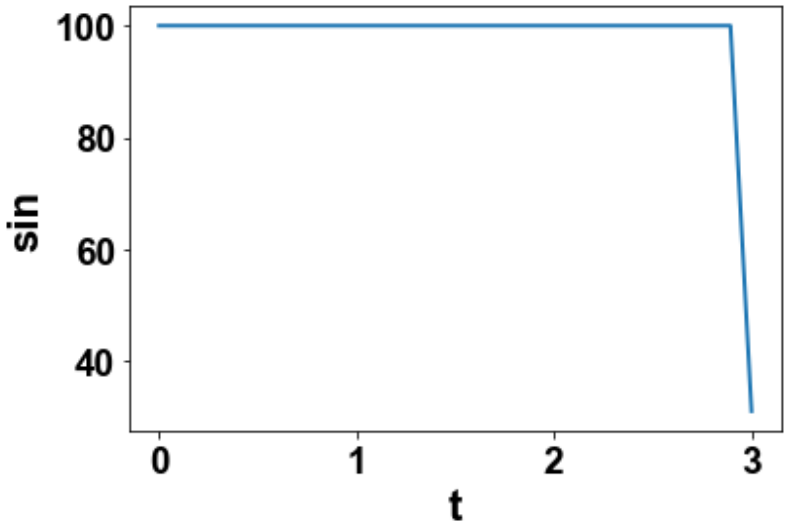

Figure 5: Droop model Sin versus t

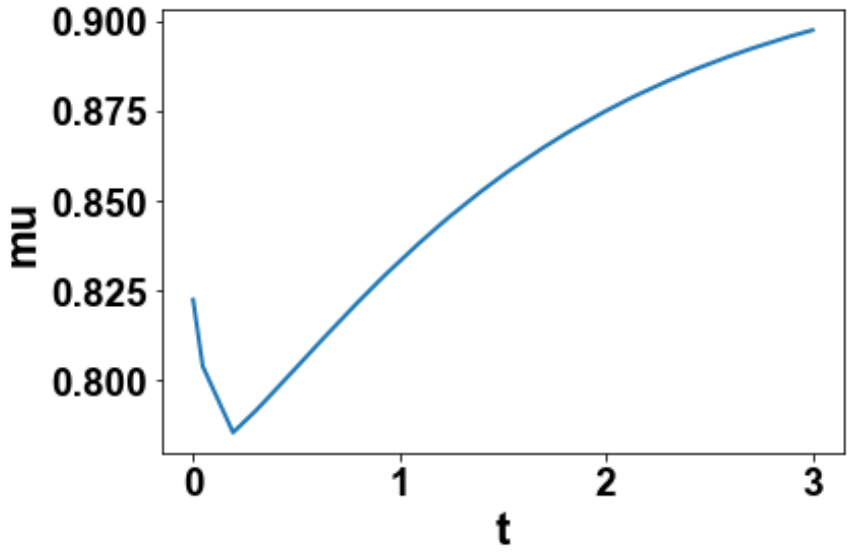

Figure 6: Droop model mu vs t

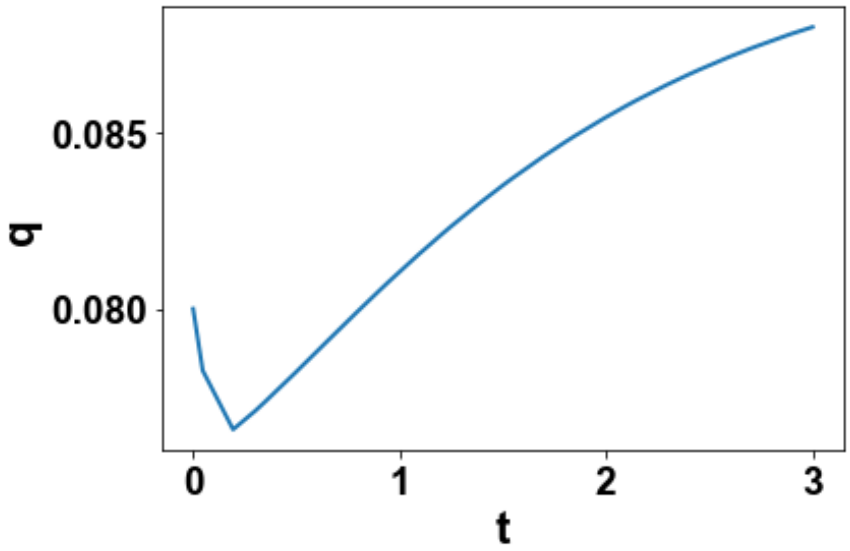

Figure 7: Droop model q vs

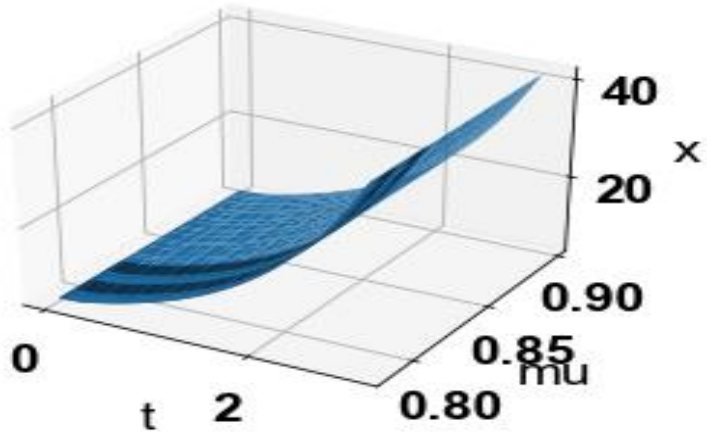

Figure 8: Droop model x t mu surface

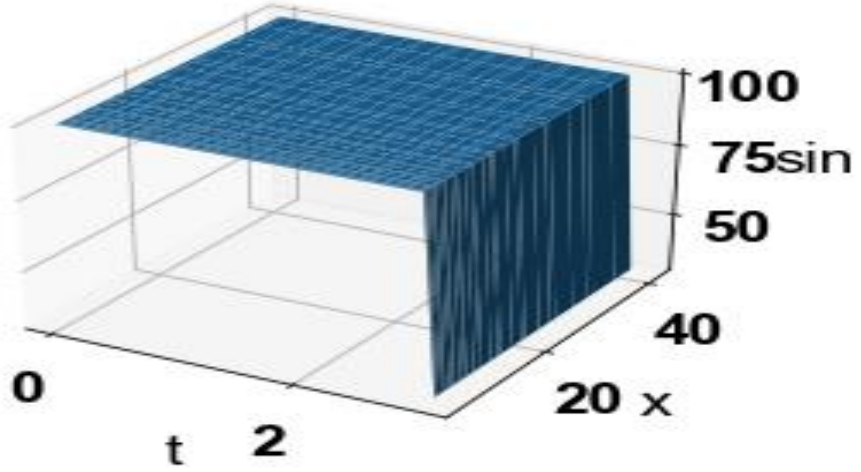

Figure 9: Droop model t x Sin surface

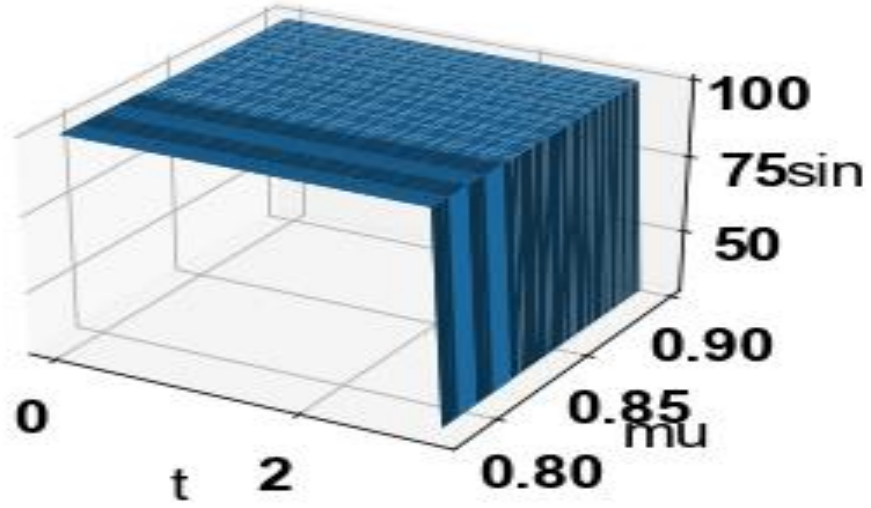

Figure 10: Droop model t mu Sin surface

3.2. Nitrogen limited MCP model

For the multiobjective nonlinear model predictive control of the nitrogen limited MCP model, the control variables are S_{in}, d and I_0. $\sum x_i$ *and* $\sum \mu_i$ are maximized individually which leads to the values 206.95 and 3.1962 respectively. The new optimization problem would be the minimization of the function $\sqrt{(\sum x_i - 206.95)^2 + (\sum \mu_i - 3.1962)^2}$ subject the equations 6-11The obtained NLMPC values of S_{in} d and I_0 were 30, 0.1 and 4.7. Figures 11-15 and figures 16a-e show the variation of the variables with time. Figs 12 and 13 show the variation of x and μ with time. While x is seen to increase μ tends to decrease with time although by a small value. Figs 11, 14 and 16(a-e) show the variation of d, *Sin* I_0 While the variation of d, and S_{in} are relatively smooth (without spikes), the variation of I_0 exhibits spikes (fig. 16a) which makes the implementation of the control difficult. In order to remedy this situation, I_0 was replaced by I_0 tanh (I_0). This replacement was not effective in removing the spikes (figs 16 b and 16 c). However, the pattern of the profiles in figures 16 b and 16c were very similar. This gave an indication that instead of by I_0 tanh, I_0 coth(I_0). would be effective. The replacement of I_0 by I_0 coth (I_0) was successful in removing the unwanted spikes that would make the implementation of the control difficult. Figures 17-21 show the Pareto surfaces for the nitrogen limited MCP model.

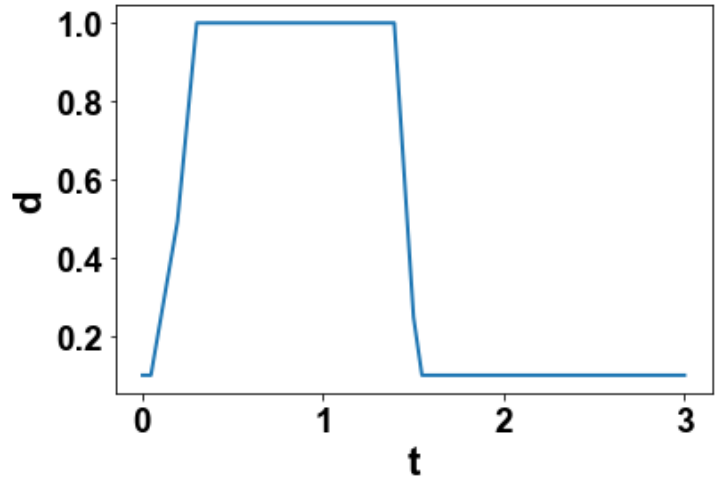

Figure 11: Nitrogen limited MCP model d versus t

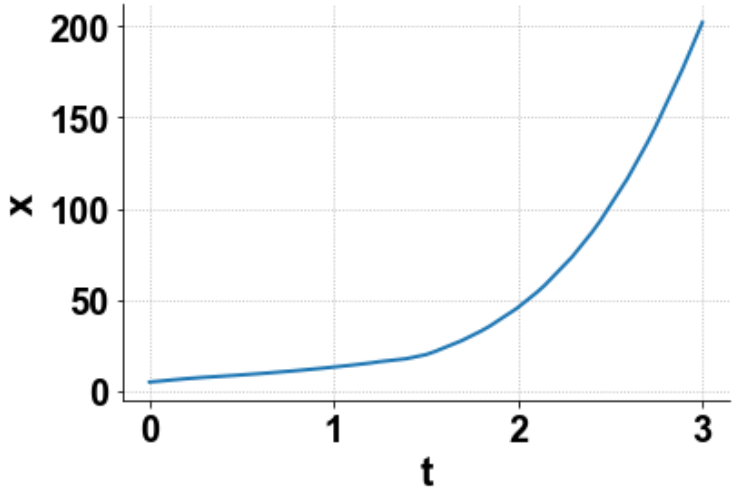

Figure 12: Nitrogen limited MCP model x versus t

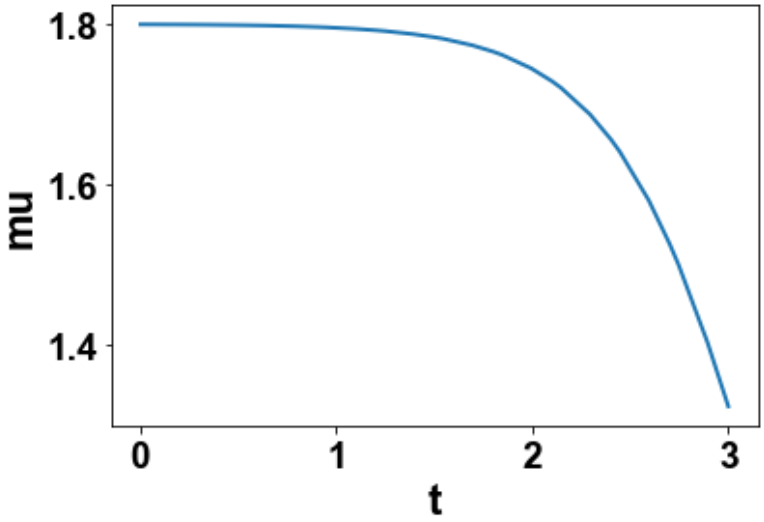

Figure 13: Nitrogen limited MCP model mu versus t

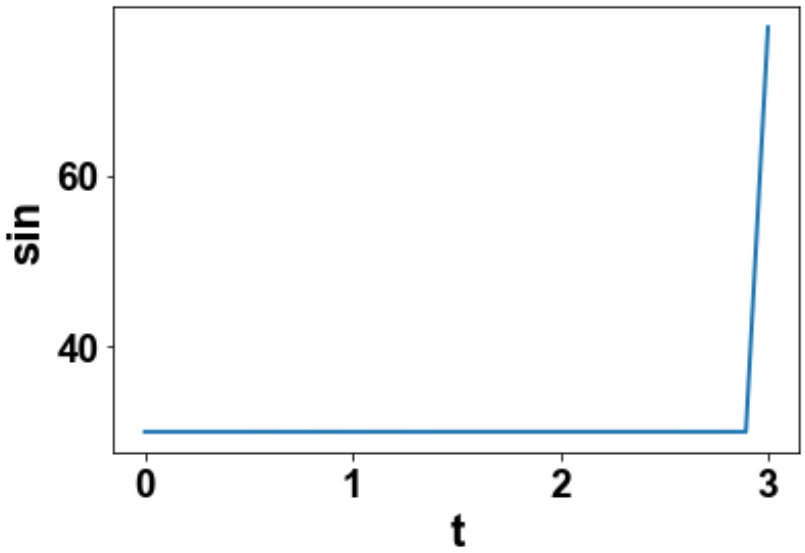

Figure 14: Nitrogen limited MCP model Sin versus t

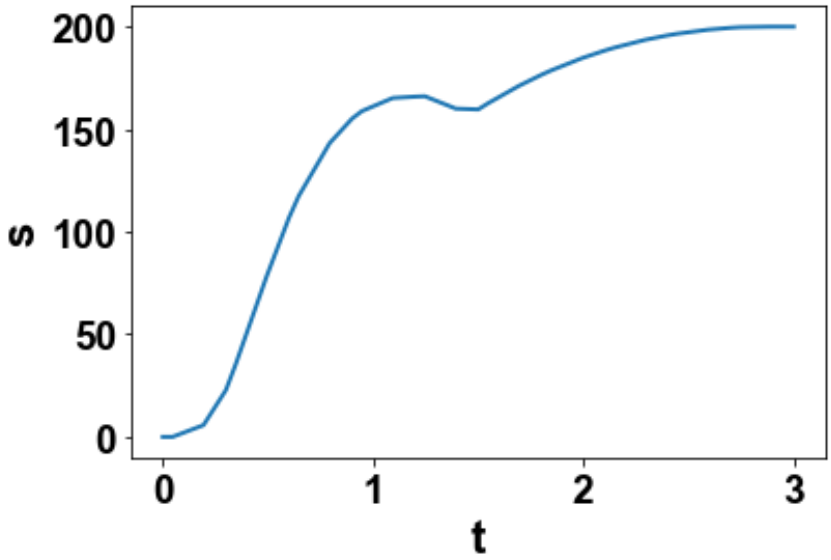

Figure 15: Nitrogen limited MCP models versus t

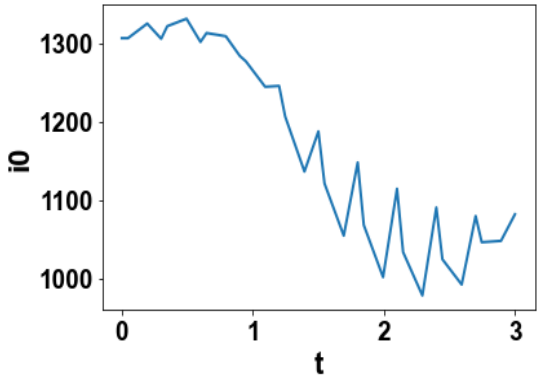

Figure 16(a): Nitrogen limited MCP model I0 vs t without activation factor

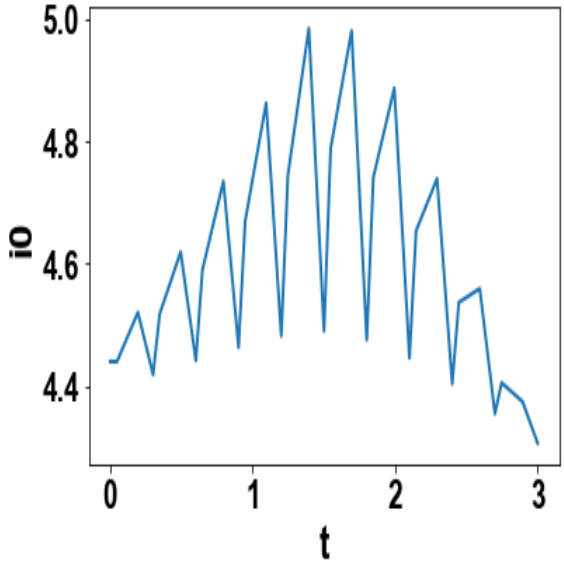

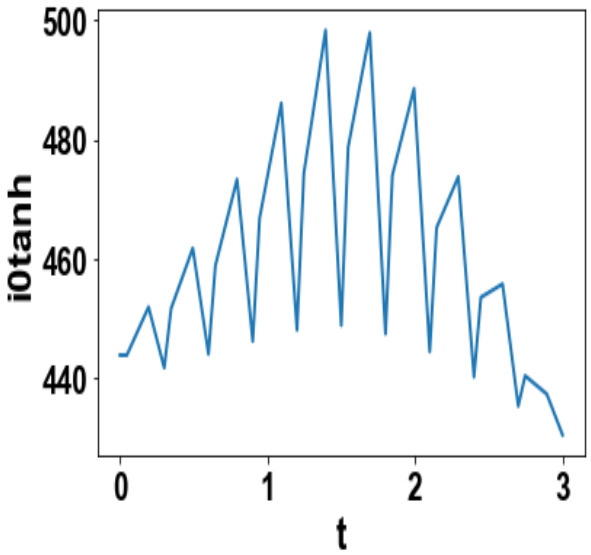

Figure 16(b and c): Nitrogen limited MCP model I0tanh(I0) as activation factor

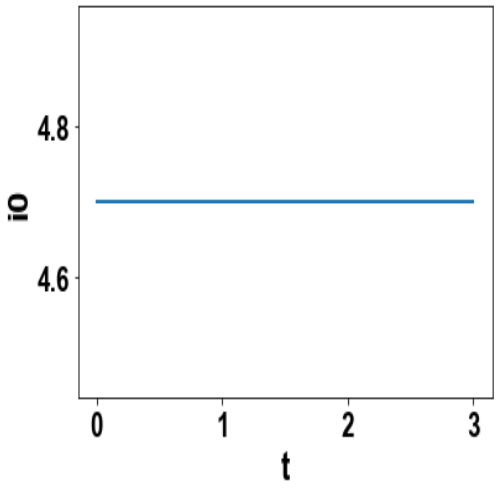

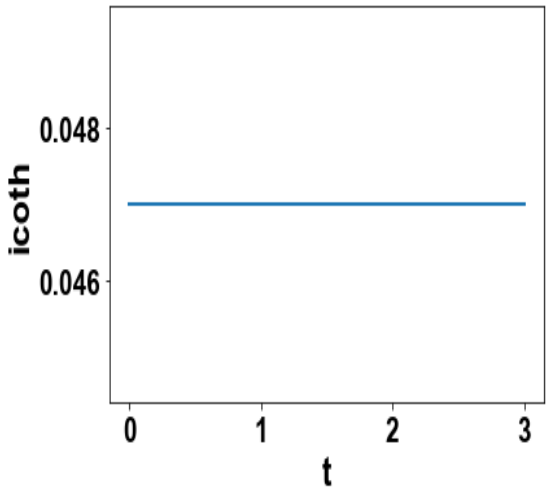

Figure 16(d and e): Nitrogen limited MCP model I0cothh(I0) as activation factor

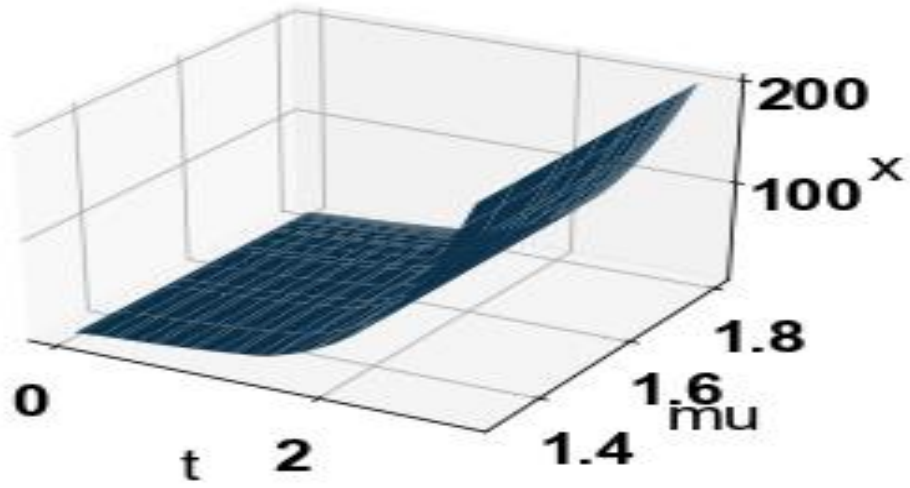

Figure 17: Nitrogen limited MCP model t x mu surface

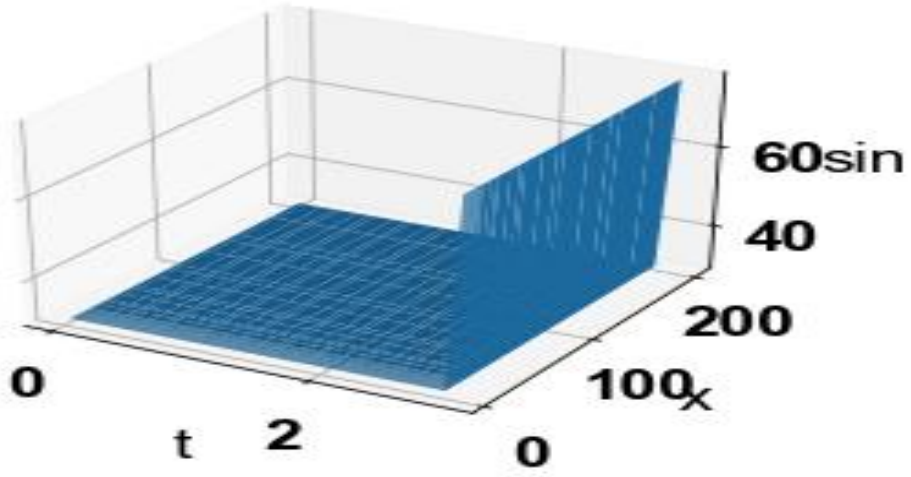

Figure 18: Nitrogen limited MCP model t x Sin surface

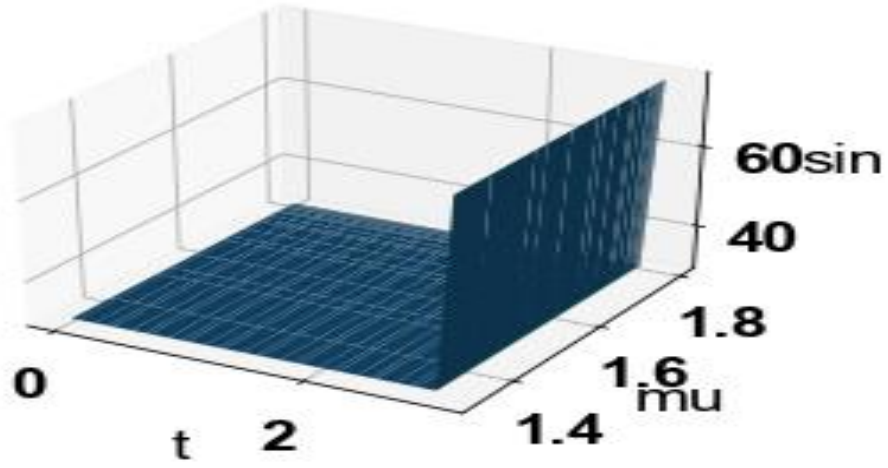

Figure 19: Nitrogen limited MCP model t mu Sin surface

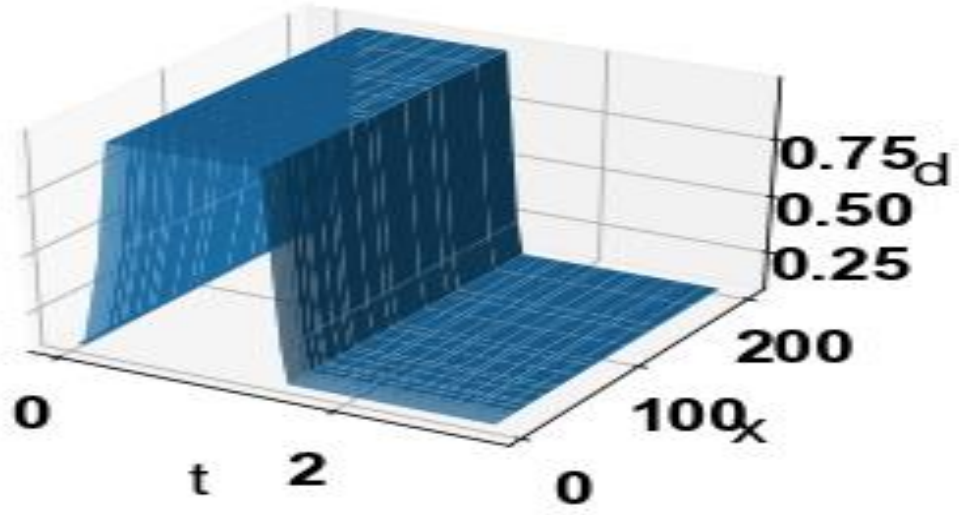

Figure 20: Nitrogen limited MCP model t x d surface

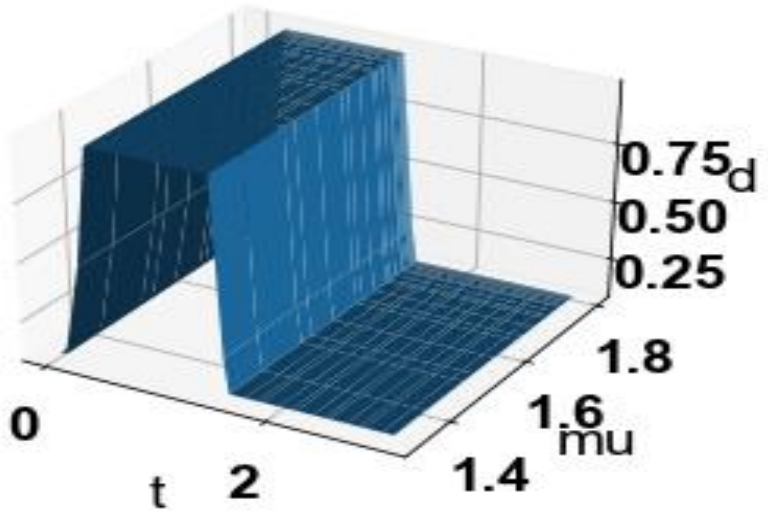

Figure 21: Nitrogen limited MCP model t mu d surface

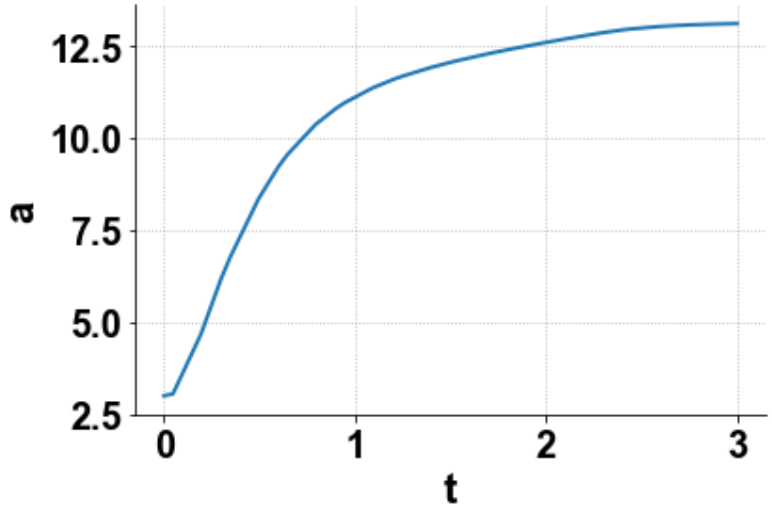

Figure 22: Thornton model a vs t

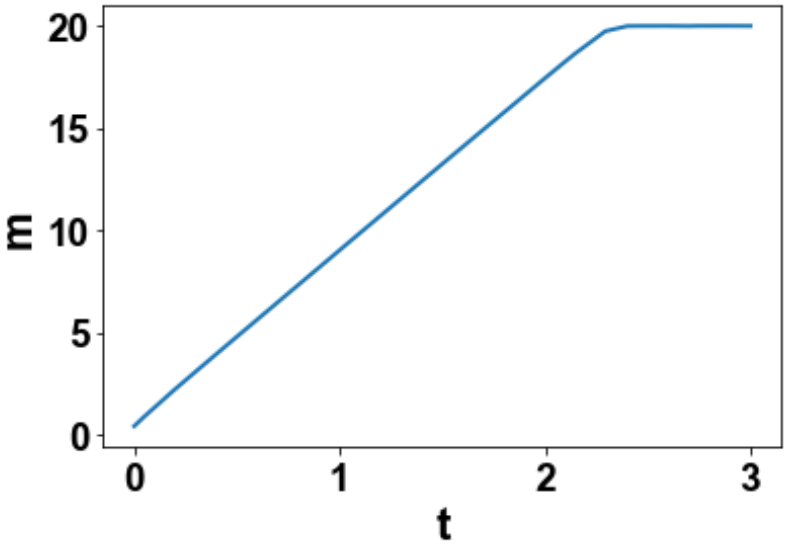

Figure 23: Thornton model m vs t

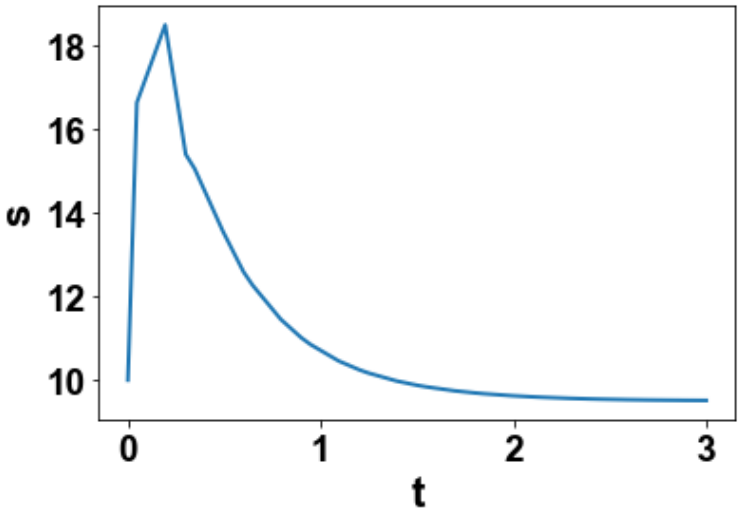

Figure 24: Thornton models vs t

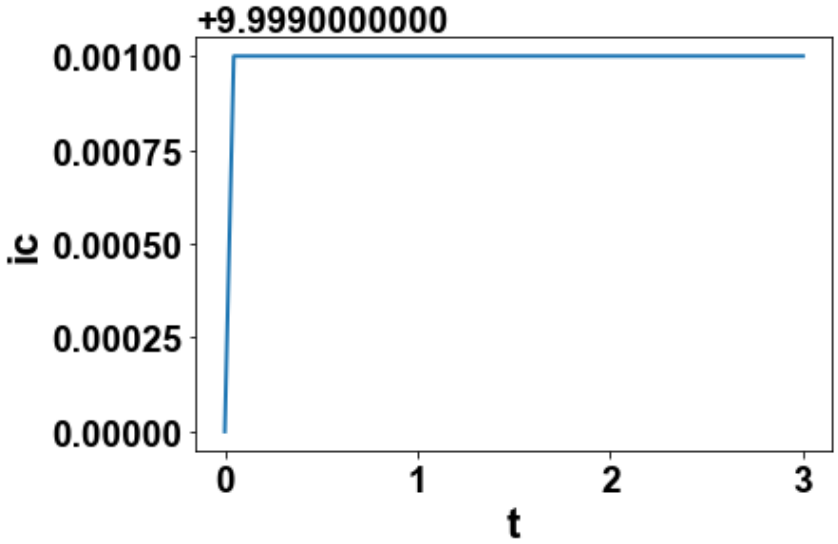

Figure 25: Thornton model ic vs t

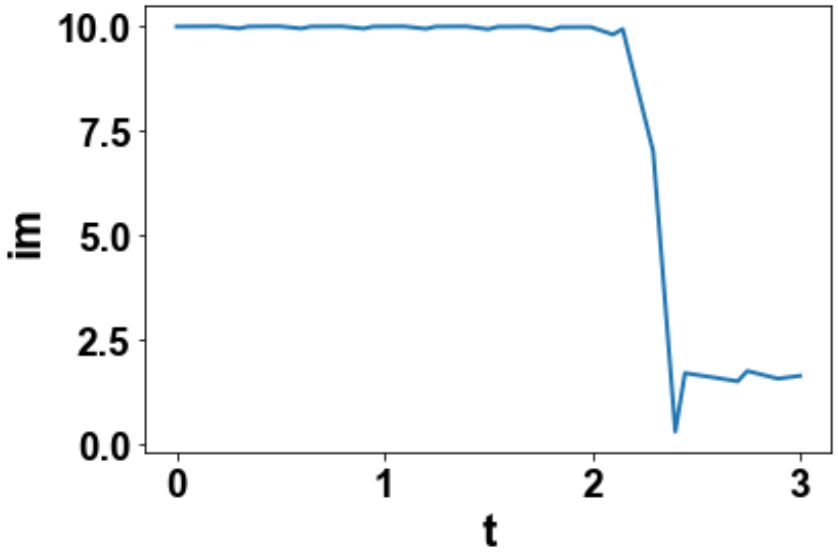

Figure 26: Thornton model im vs t

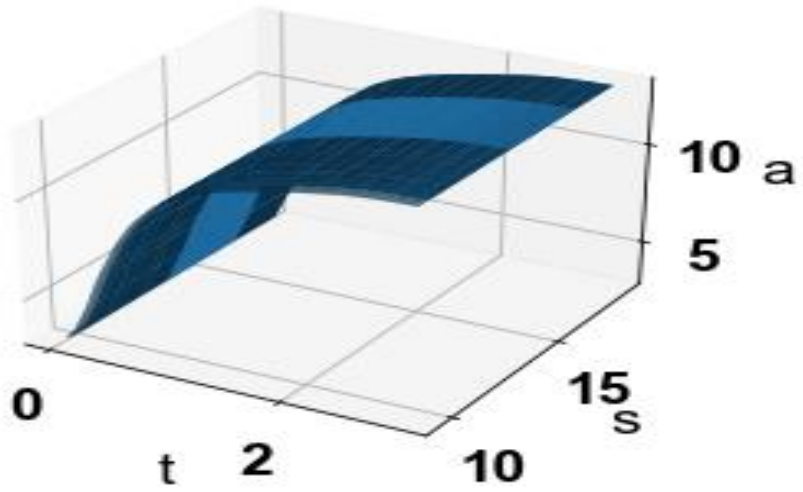

Figure 27: Thornton model a, t, s surface

3.3. Thornton Model

For the multiobjective nonlinear model predictive control of the Thornton model, the control variables are $I_c(t)$ and $I_M(t)$. $\sum A_i$ and $\sum S_i$ are maximized individually which leads to the values 16.143 and 20.1514 respectively. The new optimization problem would be the minimization of the function $\sqrt{(\sum A_i - 16.143)^2 + (\sum S_i - 20.1514)^2}$ Subject the equations 12-15. The obtained NLMPC values of I_c and I_m are 9.999 and 9.979. Figs 22-26 show the variation of the variables with time while fig 27 shows the Pareto surface. While the NLMPC procedure causes an increase in the algal biomass (fig 22), fig 24 shows an increase and a subsequent decrease in the value of the glucose concentration. This is to be expected since the growth of the algae requires the consumption of the glucose.

3.4. The main results of this work are the following

• A rigorous mulltiobjetive nonlinear model predictive control strategy was used for dynamic models involving the microalgae culture process. Three different models were used.

• These models are 1) The droop model 2) the nitrogen limited microalgae culture process model and 3) the Thornton model. It was shown that the implementation of the NLMPC method causes an increase in algal growth.

• For the nitrogen limited microalgae culture process model, the control profile (the irradiance at the surface) exhibited spikes making the implementation of the control difficult. This was remedied by using the hyperbolic cotangent function as the activation factor.

References

1. Mata, T. M., Martins, A. A., & Caetano, N. S. (2010). Microalgae for biodiesel production and other applications: a review. Renewable and sustainable energy reviews, 14(1), 217-232.
2. Soares, A. T., D'Alessandro, E. B., Lopes, R. G., Derner, R. B., & Antoniosi Filho, N. R. (2021). Optimization of biodiesel production by in situ transesterification from dry biomass of Choricystis minor var. minor via response surface methodology. Biofuels, 12(10), 1301-1307.
3. da Silva, B. F., Schmitz, J. E., Franco, I. C., & da Silva, F. V. (2021). Plantwide control systems design and evaluation applied to biodiesel production. Biofuels, 12(10), 1199-1207.
4. Humphrey, I., Chendo, M. A., Njah, A. N., & Nwankwo, D. I. (2019). Optimization of microalgae growth for biofuel production using a new empirical dynamic model. Biofuels.
5. Mondal, M., & Khan, A. A. (2021). Immobilized microalgae for removing industrial pollutants: A greener technique. In Wastewater treatment (pp. 367-384). Elsevier.
6. Enamala, M. K., Enamala, S., Chavali, M., Donepudi, J., Yadavalli, R., et al. (2018). Production of biofuels from microalgae-A review on cultivation, harvesting, lipid extraction, and numerous applications of microalgae. Renewable and Sustainable Energy Reviews, 94, 49-68.
7. Sharma, J., Kumar, S. S., Bishnoi, N. R., & Pugazhendhi, A. (2019). Screening and enrichment of high lipid producing microalgal consortia. Journal of Photochemistry and Photobiology B: Biology, 192, 8-12.
8. Sharma, J., Kumar, S. S., Bishnoi, N. R., & Pugazhendhi, A. (2018). Enhancement of lipid production from algal biomass through various growth parameters. Journal of Molecular Liquids, 269, 712-720.
9. Mathimani, T., & Mallick, N. (2018). A comprehensive review on harvesting of microalgae for biodiesel–key challenges and future directions. Renewable and Sustainable Energy Reviews, 91, 1103-1120.
10. Chu, W. L. (2017). Strategies to enhance production of microalgal biomass and lipids for biofuel feedstock. European Journal of Phycology, 52(4), 419-437.
11. Chisti, Y. (2007). Biodiesel from microalgae. Biotechnology advances, 25(3), 294-306.
12. Dugdale, R. C. J. (1967). Nutrient limitation in the sea: Dynamics, identification, and significance 1. Limnology and Oceanography, 12(4), 685-695.
13. Droop, M. R. (1970). Vitamin B 12 and marine ecology. Helgoland Marine Research, 20(1), 629-636.
14. Droop, M. R. (1983). 25 years of algal growth kinetics a personal view.

15. Thornton, A., Weinhart, T., Bokhove, O., Zhang, B., Van Der Sar, D. M., et al. (2010). Modeling and optimization of algae growth.
16. Bernard, O. (2011). Hurdles and challenges for modelling and control of microalgae for CO2 mitigation and biofuel production. Journal of Process Control, 21(10), 1378-1389.
17. Setyowati, S. Y. (2020, May). Optimal control of microalgae growth using linear quadratic regulator method with firefly algorithm optimization. In Journal of Physics: Conference Series (Vol. 1538, No. 1, p. 012047). IOP Publishing.
18. Flores-Tlacuahuac, A., Morales, P., & Rivera-Toledo, M. (2012). Multiobjective nonlinear model predictive control of a class of chemical reactors. Industrial & Engineering Chemistry Research, 51(17), 5891-5899.
19. Sridhar, L. N. (2022). Multiobjective optimization and nonlinear model predictive control of the continuous fermentation process involving Saccharomyces Cerevisiae. Biofuels, 13(2), 249-264.
20. Miettinen, K. (1999). Nonlinear multiobjective optimization (Vol. 12). Springer Science & Business Media.
21. Hart, W. E., Laird, C. D., Watson, J. P., Woodruff, D. L., Hackebeil, G. A., et al. (2017). Pyomo-optimization modeling in python (Vol. 67, p. 277). Berlin: Springer.
22. Biegler, L. T. (2007). An overview of simultaneous strategies for dynamic optimization. Chemical Engineering and Processing: Process Intensification, 46(11), 1043-1053.
23. Wächter, A., & Biegler, L. T. (2006). On the implementation of an interior-point filter line-search algorithm for large-scale nonlinear programming. Mathematical programming, 106, 25-57.
24. Tawarmalani, M., & Sahinidis, N. V. (2005). A polyhedral branch-and-cut approach to global optimization. Mathematical programming, 103(2), 225-249.